

Contents

[Contributors](#)

[Prologue](#)

[Preface](#)

SECTION I PERIOPERATIVE MANAGEMENT

1. [Echocardiography for cardiac surgery](#)
Jared W. Feinman, Bonnie L. Milas, and Joseph S. Savino
2. [Cardiopulmonary bypass: access, technical options and pathophysiology](#)
Jack H. Boyd and Albert J. Pedroza
3. [Circulatory arrest: retrograde vs antegrade cerebral protection](#)
Joshua M. Rosenblum and Edward P. Chen
4. [Intraoperative myocardial protection](#)
Richard D. Weisel and Terrence M. Yau

SECTION II SURGERY FOR ISCHEMIC HEART DISEASE

5. [On-pump coronary artery bypass grafting](#)
Marvin D. Atkins and Matthew L. Williams
6. [Off-pump coronary revascularization](#)
Gianluca Torregrossa, Timothy Lee, and John D. Puskas
7. [Expanded use of arterial conduits](#)
Philip A.R. Hayward, Sean D. Galvin, and Brian F. Buxton
8. [Reoperative coronary artery bypass grafting](#)
Murray H. Kwon and Richard J. Shemin
9. [Repair of postinfarction ventricular septal defect](#)
Cynthia E. Wagner and Irving L. Kron
10. [Robotic total endoscopic coronary artery bypass grafting](#)
László Göbölös and Johannes Bonatti

SECTION III SURGERY FOR VALVULAR HEART DISEASE

11. [Aortic valve replacement](#)
Ismail El-Hamamsy, Maxime Laflamme, and Louis P. Perrault
12. [Minimal access aortic valve surgery](#)

- Elizabeth H. Stephens and Michael A. Borger*
13. TAVR: transfemoral and alternative approaches
Chase R. Brown and Wilson Y. Szeto
14. Aortic valve repair
George J. Arnaoutakis and Joseph E. Bavaria
15. Mitral valve replacement
T. Sloane Guy
16. Mitral valve repair
Javier G. Castillo and David H. Adams
17. Minimal access mitral valve surgery
Arman Kilic, Pavan Atluri and W. Clark Hargrove III
18. Robot-assisted mitral valve surgery
Kaushik Mandal and W. Randolph Chitwood Jr.
19. Tricuspid valve surgery
Takeyoshi Ota and Valluvan Jeevanandam
20. The pulmonary autograft for aortic valve replacement
Zohair Y. Al Halees
21. Valvular endocarditis
Nishant Saran and Alberto Pochettino
22. Valve-sparing aortic root replacement
Ibrahim Sultan and Thomas G. Gleason

SECTION IV SURGERY FOR HEART FAILURE

23. Heart transplantation
Arman Kilic and Pavan Atluri
24. Heart–lung transplantation
Christian A. Bermudez
25. Lung transplantation
Edward Cantu
26. Permanent continuous-flow left ventricular assist devices
Erin M. Schumer and Mark S. Slaughter
27. ECMO and temporary mechanical circulatory assistance
Christian A. Bermudez and Jeffrey Poynter
28. Left ventricular reconstruction
Edwin C. McGee Jr. and Patrick M. McCarthy
29. Surgery for hypertrophic cardiomyopathy
Robert J. Steffen and Nicholas G. Smedira
30. Congestive heart failure: surgical techniques for functional mitral regurgitation
Sarah T. Ward, Alexander A. Brescia, Matthew A. Romano, and Steven F. Bolling

SECTION V THORACIC AORTIC DISEASE

31. Ascending aortic aneurysm
Ryan P. Plichta and G. Chad Hughes
32. Hybrid aortic arch repair
Daniel-Sebastian Dohle and Nimesh D. Desai
33. Thoracoabdominal aortic aneurysms
Shinichi Fukuhara and Nimesh D. Desai
34. Thoracic endovascular aortic repair
George J. Arnaoutakis and Wilson Y. Szeto
35. Aortic dissection: type A and B
Arman Kilic and Prashanth Vallabhajosyula

SECTION VI SURGERY FOR CARDIAC RHYTHM DISORDERS AND TUMORS

36. The cut-and-sew Maze-III procedure for the treatment of atrial fibrillation
James L. Cox
37. Cardiac tumors
Gabriel S. Aldea and Edward D. Verrier
38. Pacers—BV pacers
Michael J. Grushko, Andrew Krumerman, and Joseph J. DeRose Jr.

SECTION VII SURGERY FOR CONGENITAL HEART DISEASE

39. The anatomy of congenital cardiac malformations
Robert H. Anderson and Diane E. Spicer
40. Palliative procedures: shunts and pulmonary artery banding
David P. Bichell
41. Total anomalous pulmonary venous connection and cor triatriatum
Jennifer C. Romano and Edward L. Bove
42. Atrial septal defects
Peter B. Manning
43. Atrioventricular septal defects
Michael O. Murphy and Thomas L. Spray
44. Bidirectional Glenn and hemi-Fontan procedures
J. Mark Redmond
45. Fontan procedure for functionally single ventricle and double-inlet ventricle
Tara Karamlou and Gordon A. Cohen
46. Double-outlet ventricles
Pascal Vouhé, Olivier Raisky, and Yves Lecompte
47. Ebstein's malformation of the tricuspid valve: surgical treatment and the cone repair

- Jose Pedro Da Silva*
48. Ventricular septal defect
Carl Lewis Backer
49. Tetralogy of Fallot
Tom R. Karl and Nelson Alphonso
50. Pulmonary atresia with ventricular septal defect
V. Mohan Reddy and Frank L. Hanley
51. Right ventricular outflow tract obstruction with intact ventricular septum
Stephanie Fuller
52. Left ventricular outflow tract obstruction
Ross M. Ungerleider and Irving Shen
53. Transposition of the great arteries with left ventricular outflow tract obstruction
Christo I. Tchervenkov and Pierre-Luc Bernier
54. Transposition of the great arteries with right ventricular outflow tract obstruction
Ergin Kocyildirim, Mahesh S. Sharma, and Victor O. Morell
55. Anatomical repair of transposition of the great arteries
Francois Lacour-Gayet
56. Congenitally corrected transposition
David J. Barron
57. Persistent truncus arteriosus
Martin J. Elliott and Victor T. Tsang
58. Persistent ductus arteriosus
William M. DeCampli
59. Aortopulmonary window
William M. DeCampli
60. Coarctation of the aorta: repair of coarctation and arch interruption
Christopher E. Mascio and Erle H. Austin III
61. Congenital anomalies of the aortic arch
Nhue Do, Luca Vricella, and Duke E. Cameron
62. Hypoplastic left heart syndrome
Aaron Eckhauser and Thomas L. Spray
63. Coronary anomalies
Julie Brothers and J. William Gaynor
64. Cardiac transplantation for congenital heart disease
James A. Quintessenza
65. Lung and heart–lung transplantation for congenital heart disease
Charles B. Huddleston and Andrew C. Fiore
66. Ventricular assist devices for congenital heart disease
David L.S. Morales, Farhan Zafar, and Charles D. Fraser Jr.
67. Congenital mitral valve repair

Vladimiro L. Vida, Massimo A. Padalino, and Giovanni Stellin

68. Aortic valve repair

Emile Bacha and Paul Chai

Index

Echocardiography for cardiac surgery

JARED W. FEINMAN, BONNIE L. MILAS, AND JOSEPH S. SAVINO

HISTORY

The ability to perform real-time cardiovascular imaging in the operating room using transesophageal echocardiography (TEE) has been the most important diagnostic advancement in cardiac surgery over the past 30 years. TEE was developed in the mid 1970s but did not enter widespread use until the early 1980s when flexible TEE probes with manipulatable tips became available. The early probes were only capable of imaging along a single plane (monoplane), which somewhat limited their utility. The technology behind ultrasound image acquisition has moved forward rapidly, however, to the point that modern TEE probes can image along a 180 degree axis, display multiple imaging planes simultaneously (x plane imaging) and acquire large pyramids of data that allow real-time, three-dimensional (3D) rendering of cardiac structures. As intraoperative TEE use has become commonplace, there has been a joint effort by the American Society of Echocardiography (ASE) and the Society of Cardiovascular Anesthesiologists (SCA) to standardize the perioperative TEE examination through the issuance of joint guideline statements as well as the establishment of a board certification process administered by the non-profit National Board of Echocardiography. The first set of guidelines on performing a comprehensive TEE exam was issued in 1999, and consisted of 20 standard echocardiographic views. This was expanded to 28 two-dimensional (2D) views and a focused 3D exam in the most recent 2013 update. Current recommendations state that an intraoperative TEE should be performed (barring a contraindication) in all patients undergoing open heart, thoracic aorta, or catheter-based cardiac surgery, in most patients having coronary artery bypass grafting (CABG), and in any patients having non-cardiac surgery with known or suspected cardiac pathology that may impact outcomes.

PRINCIPLES AND JUSTIFICATION

A few general principles regarding image generation, interpretation of data, and limitations of the ultrasound system are useful in understanding TEE in the operating room. In basic terms, the ultrasound transducer uses piezoelectric crystals to convert electrical energy into high-frequency

acoustic energy (ultrasound waves) and vice versa. The ultrasound waves that are emitted from the transducer travel through tissue planes where they can be absorbed (converted into heat), refracted (if crossing between objects with different propagation speeds), or reflected (if adjacent media have different acoustic impedances) back towards the probe where they are converted by the ultrasound system into an image. Since reflection occurs best at a 90-degree angle, 2D imaging will be most effective when the ultrasound beam is orthogonal to the tissue being imaged. Also, any material that causes a lot of reflection (e.g. prosthetic valves and calcium deposits) will not allow the ultrasound beam to pass beyond it, impairing the ability to image more distant structures. The data being reflected back to the ultrasound probe can be expressed in two different imaging formats. The most common is 2D B-mode imaging, where a line of echo data is moved back and forth in an arc through a section of tissue and displayed so that a continuous 2D image is generated. Alternatively, in M-mode imaging a single scan line is displayed over time, which allows for a very high frame rate and accuracy of linear measurements. Modern, full matrix array transducers have about 3000 independent piezoelectric elements that can be fired in a phased manner to generate a radially propagating scan line. The scan line can be steered in three planes to generate a true 3D volume of data, which can either be displayed in real time or stitched together with adjoined volumes using ECG-gating to produce an even larger volume of 3D data.

Doppler ultrasound can be used to assess the velocity of blood flow or tissue movement within the heart and vascular structures. Since this form of imaging relies on the Doppler shift equation:

$$\text{Doppler shift} = (2 \times \text{velocity of object} \times \text{incident frequency} \times \cosine \theta) \text{ Propagation speed of ultrasound}$$

a calculated velocity will be most accurate when the ultrasound beam is perfectly aligned with the blood flow being assessed ($\cosine 0^\circ = 1$), and should only be used if θ is <20 degrees. This stands in contrast to the aforementioned 2D imaging, which will achieve the best resolution when the structure being imaged is orthogonal to the ultrasound beam. Doppler imaging is used in three common modes: pulsed-wave Doppler, continuous-wave Doppler, and color-flow Doppler. Pulsed-wave and continuous-wave Doppler imaging both assess the velocity of the object being imaged over time, but differ in that the former is limited in the maximum velocity that can be assessed (Nyquist limit) but has range specificity, while the latter is not limited by a maximum velocity but has range ambiguity. Thus, pulsed-wave Doppler is used to assess low-velocity flow in a specific location (e.g. pulmonary vein flow, transmitral inflow in a non-stenotic valve) while continuous-wave Doppler is useful in assessing high-velocity flow through a stenotic or regurgitant valve. Color-flow Doppler imaging overlays pulsed-wave Doppler data on a standard 2D image to generate a color map that provides information on the direction of blood flow as well as semi-quantitative information on the mean velocities of flow. Traditionally, blue denotes movement away from the ultrasound probe and red movement towards the probe.

The TEE probe itself is essentially a modified gastroscope with a matrix array of piezoelectric

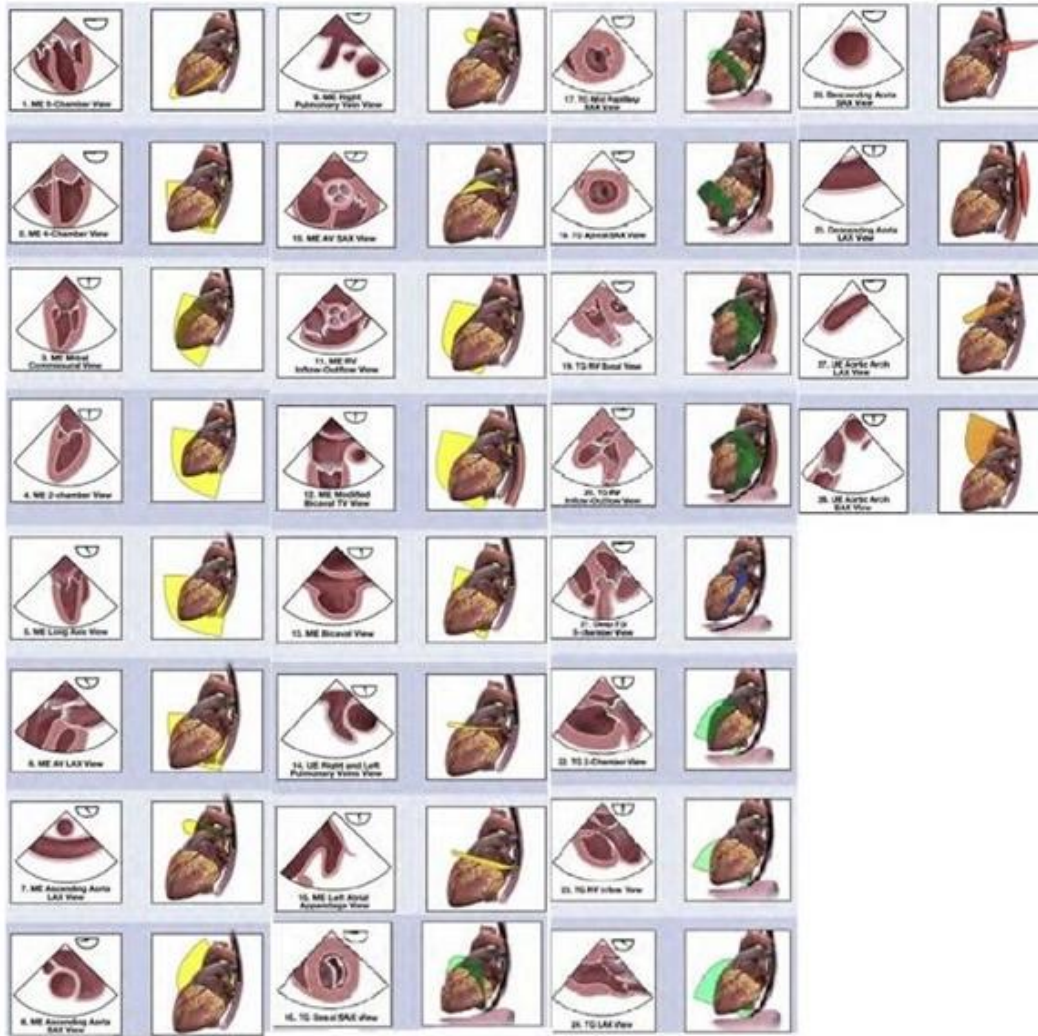
crystals at the tip in place of a camera. Probe insertion and manipulation may lead to significant injury, and precautions are necessary to minimize the risk. Most perioperative TEEs are performed in anesthetized and intubated patients who cannot respond to pain or discomfort caused by excessive probe impingement of soft tissue. Before insertion, the TEE probe is inspected for damage or any break in the encasement. Then the probe is lubricated, inserted into the mouth, and passed posteriorly into the esophagus, and most imaging occurs at the level of the midesophagus, upper esophagus, or stomach. Manufacturers' recommendations for probe cleaning and maintenance should be followed with a systematic approach to instrument processing. Complications from probe insertion are uncommon (0.2% in one case series of 7200 patients reported by Kallmeyer et al.), and range from minor trauma to the teeth or pharynx to esophageal perforation, which carries with it a high risk of mortality.

Contraindications to TEE are disorders of the mouth, esophagus, or stomach that could preclude safe passage of the probe. These include esophageal strictures, diverticula, or webs, cancerous masses, or an active esophageal perforation or bleed. Abnormal displacement of the esophagus, such as may occur with a large aortic aneurysm, is not a contraindication, but is associated with increased risk. In patients where there is a question of esophageal disease, the risks and benefits of TEE for that specific procedure must be weighed. If TEE is to be performed, it may be prudent to first have an esophagogastroduodenoscopy (EGD) done in the operating room to make sure that placement is safe, and/or to use a pediatric TEE probe, which is much smaller in diameter than a standard adult probe but comes with significant imaging limitations.

COMPREHENSIVE TEE EXAMINATION

The current ASE/SCA guideline statement on performing a comprehensive TEE examination lists 28 standard views with additional 2D and 3D imaging performed as needed (see **Figure 1.1**). The TEE probe is initially inserted to a depth of approximately 30 cm and the entirety of the examination is performed by adjusting the rotation of the beam within the probe (omniplane angle), rotating the probe itself to the left or right, or moving the probe farther into or out of the esophagus/stomach. The views and the corresponding approximate omniplane angle (between 0° and 180°) for each view are illustrated in the figure. The order in which a TEE exam is conducted varies between individual providers. While there is no “ideal” order of imaging, it is important for an echocardiographer to choose a protocol and follow it in every case, as this will prevent any unanticipated findings from being missed. When discussing standard TEE views, the nomenclature is such that each view is named for the location of the probe in space (e.g. upper esophageal (UE), midesophageal (ME), or transgastric (TG)) followed by what is being imaged (four-chamber, two-chamber, etc.). **Figure 1.1** has been reproduced with permission from Hahn RT, Abraham T, Adams MS, et al. Guidelines for performing a comprehensive transesophageal echocardiographic examination: recommendations from the American Society

of Echocardiography and the Society of Cardiovascular Anesthesiologists. *J Am Soc Echocardiogr.* 2013; 26: 921–64.



1.1 TEE examination standard views.

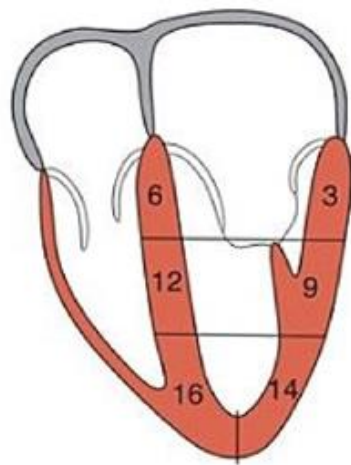
Left ventricle

The left ventricle (LV) can be divided into a series of segments that allows correlation of regional wall motion with abnormalities in coronary blood flow. There are currently two commonly used models of left ventricular anatomy: the 16-segment model and the 17-segment model. The only difference between the two is that the former divides the apex of the heart into

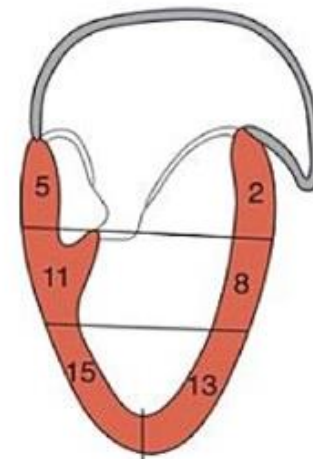
anterior, lateral, inferior, and septal regions, while the latter adds a fifth segment, the apical cap, made up of the myocardium beyond the end of the LV cavity.

The longitudinal axis of the LV is described as basal, mid, or apical. The midesophageal four-chamber view shows the three inferoseptal and three anterolateral segments (**Figure 1.2a**). Midesophageal two-chamber views show the three anterior and three inferior segments (**Figure 1.2b**) and midesophageal long-axis (LAX) views show the two anteroseptal and two inferolateral segments (**Figure 1.2c**). TG short-axis (SAX) views show all six segments at the mid (**Figure 1.2d**) and basal (**Figure 1.2e**) levels, and all four segments at the apical level. These figures have been reproduced with permission from Shanewise JS, Cheung AT, Aronson S, et al. ASE/SCA guidelines for performing a comprehensive intraoperative multiplane transesophageal echocardiography examination: recommendations of the American Society of Echocardiography Council for Intraoperative Echocardiography and the Society of Cardiovascular Anesthesiologists Task Force for Certification in Perioperative Transesophageal Echocardiography. *Anesth Analg*. 1999; 89: 870–84, and *J Am Soc Echocardiogr*. 1999; 12: 884–900.

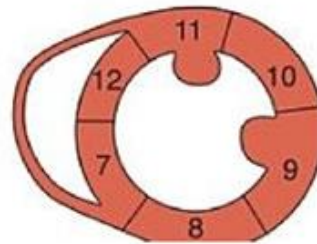
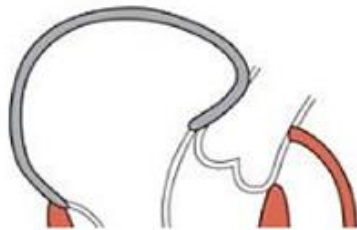
See also **Figures 1.3–1.7**.

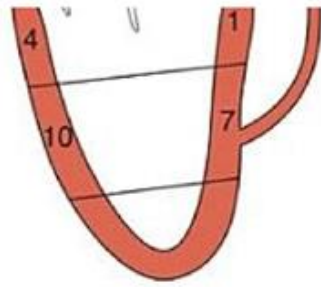


a. ME four-chamber view



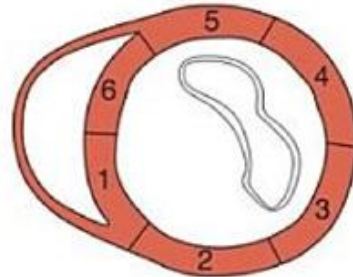
b. ME two-chamber view





c. ME long-axis view

d. TG mid-short-axis view



e. TG basal short-axis view

Key

Basal segments

- 1 = Basal anteroseptal
- 2 = Basal anterior
- 3 = Basal anterolateral
- 4 = Basal inferolateral
- 5 = Basal inferior
- 6 = Basal inferoseptal

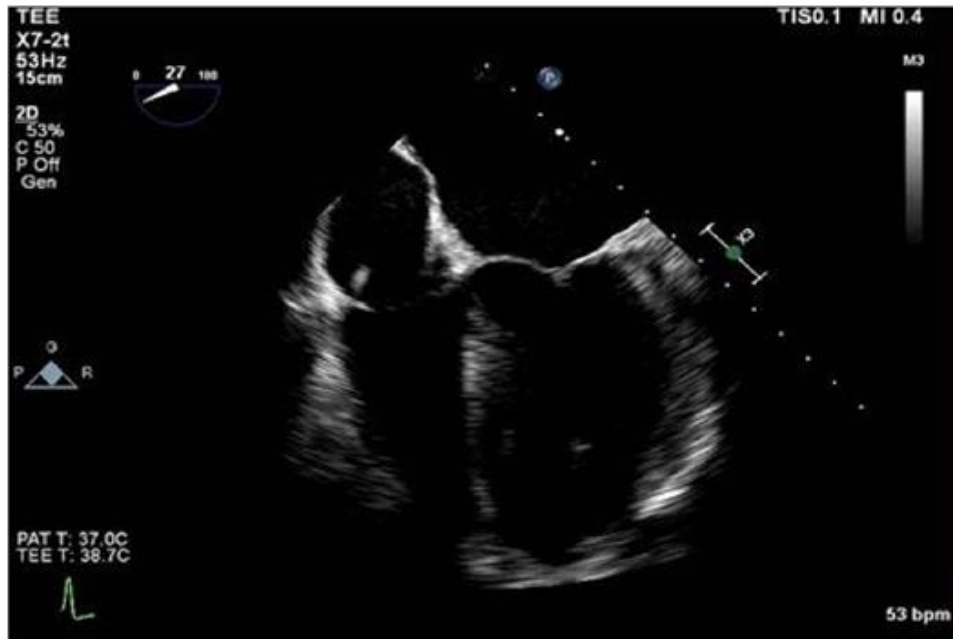
Mid segments

- 7 = Mid anteroseptal
- 8 = Mid anterior
- 9 = Mid anterolateral
- 10 = Mid inferolateral
- 11 = Mid inferior
- 12 = Mid inferoseptal

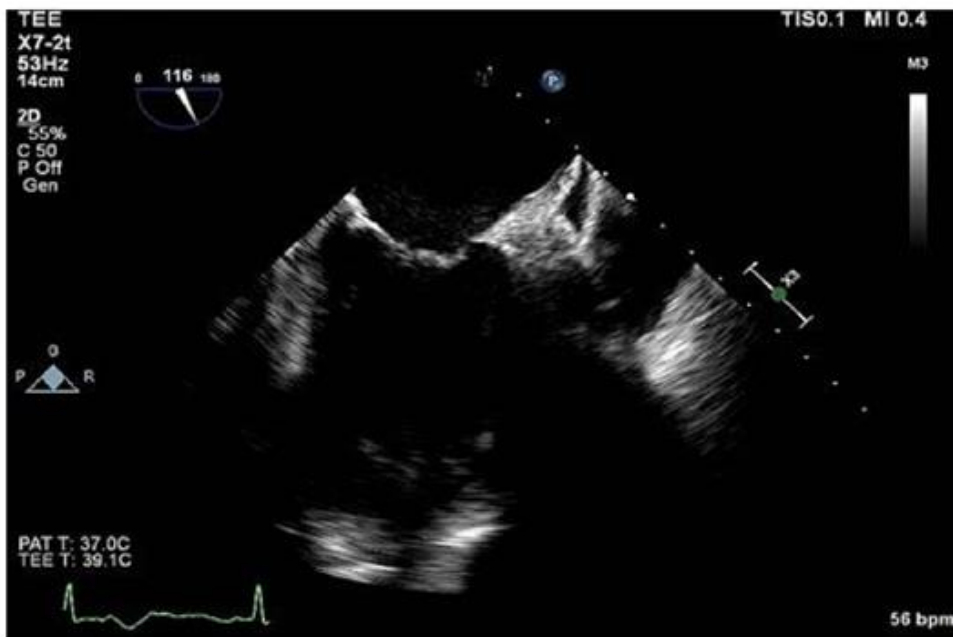
Apical segments

- 13 = Apical anterior
- 14 = Apical lateral
- 15 = Apical inferior
- 16 = Apical septal

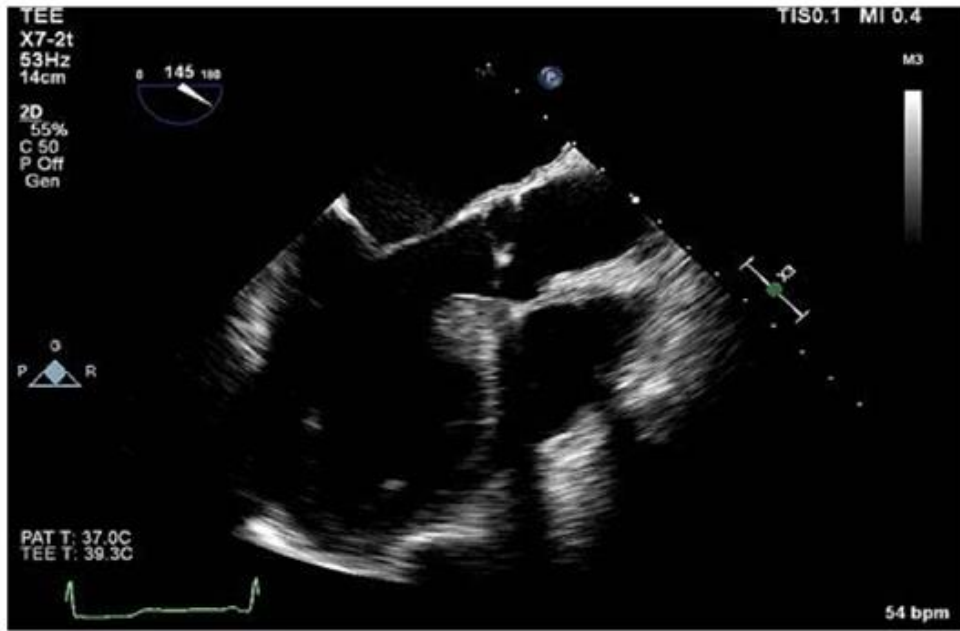
1.2a-e



1.3 LV midesophageal four-chamber view.



1.4 LV midesophageal two-chamber view.



1.5 LV midesophageal long-axis view.

